Enhanced photocatalytic removal of phenol from aqueous solutions using ZnO modified with Ag

V. Vaiano[a,*], M. Matarangolo[a], J.J. Murcia[b], H. Rojas[b], J.A. Navío[c], M.C. Hidalgo[c]

[a] Department of Industrial Engineering, University of Salerno, via Giovanni Paolo II, 132, 84084 Fisciano, SA, Italy
[b] Grupo de Catálisis, Escuela de Ciencias Químicas, Universidad Pedagógica y Tecnológica de Colombia UPTC, Avenida Central del Norte, Tunja, Boyacá, Colombia
[c] Instituto de Ciencia de Materiales de Sevilla (ICMS), Consejo Superior de Investigaciones Científicas CSIC–Universidad de Sevilla, Américo Vespucio 49, 41092 Sevilla, Spain

ARTICLE INFO

ABSTRACT

Different photocatalysts based on commercial ZnO modified by silver photodeposition were prepared in this work. The samples were characterized by X-ray fluorescence spectrometry (XRF), specific surface area (SSA), transmission electron microscopy (TEM), X-ray photoelectron spectroscopy (XPS), X-ray diffraction (XRD) and UV–vis diffuse reflectance (UV–vis DRS). XRD and XPS showed that Ag/ZnO samples are composed of metallic Ag (Ag^0) and ZnO structure was identified. Furthermore, TEM analysis evidenced that the number of silver particles increased with the Ag content. At last, UV–vis DRS results revealed a reflectance band for Ag/ZnO samples, ascribed to the surface plasmon resonance (SPR) absorption of metal silver particles. Commercial ZnO and Ag/ZnO samples were evaluated in the phenol removal under UV light irradiation. It was observed an enhancement of photocatalytic phenol removal from aqueous solutions by silver addition in comparison to commercial ZnO. In particular, the phenol removal increased with the silver content from 0.14 to 0.88 wt%, after this content (i.e 1.28 wt%) the phenol degradation significantly decreased indicating that the optimal Ag content was equal to 0.88 wt%. The influence of the best photocatalyst dosage and the change of the initial phenol concentration in solution were also investigated in this work and the best photocatalytic performance was obtained by using 50 mg L^{-1} of phenol initial concentration and 0.15 g L^{-1} of photocatalyst dosage. Finally, the optimized Ag/ZnO photocatalyst was employed for the treatment of a real drinking wastewater containing phenol in which the almost total phenol removal was achieved after 180 min of UV irradiation time.

1. Introduction

Phenol and phenolic compounds are considered as priority pollutants since they are dangerous for living organisms due to their acute toxicity and bio-recalcitrant nature [1,2]. These compounds are released into the environment through wastewaters from a large number of industries, such as tanning, refineries, manufacturing paints, pharmaceuticals, petroleum production, paper making, coke and iron-smelting processes [3–7]. Phenol and its derivatives were found in concentrations of more than 1 mg L^{-1} in different industrial wastewaters and because of its stability and solubility in water, it is difficult to reduce its concentration up to the security level (0.1–1 mg L^{-1}) [6,8]. For this reason, International Organizations for Environmental Protection have established permissible limits, in the order of a few micrograms per liter, for their discharge into the environment [9]. However, it is difficult to eliminate the phenol with conventional treatment processes; in particular, the biological process is usually

ineffective because of a self-inhibitory effect on the microorganisms in the presence of phenolic compounds [10]. For this reason, photocatalytic treatment represents an advanced oxidation technology able to remove organic pollutants thanks to its extremely efficient degradation rate, high mineralization efficiency, leading to CO_2, H_2O, and other minerals as final products [11–17]. In particular, photocatalysis has been extensively investigated as a technology for the removal of phenol and phenolic compounds from waters [18,19]. Among various semiconductor materials, ZnO have received considerable scientific interest as an alternative to TiO_2 due to its remarkable performance in electronics, optics and photonics, non-toxicity, low cost, high catalytic efficiency, wide band gap energy (3.37 eV at room temperature), large exciton binding energy (60 meV) and high potential to adsorb UV light irradiation. In some cases, it was also reported that ZnO was more efficient than TiO_2 in photocatalytic degradation of some organic compounds in aqueous solution [18,20,21]. The use of ZnO was investigated in the photocatalytic degradation of phenolic compounds

Table 1
List of synthetized photocatalysts and their characteristics.

	Commercial ZnO	0.25%Ag/ZnO	0.5%Ag/ZnO	0.75%Ag/ZnO	1%Ag/ZnO	2%Ag/ZnO
Nominal Ag loading [wt%]	–	0.25	0.5	0.75	1	2
Measured Ag loading [wt%]	–	0.14	0.38	0.57	0.88	1.28
Crystallite size [nm]	24	24	24	24	24	24
Band gap [eV]	3.1	3.1	3.1	3.1	3.1	3.1
SSA [m^2/g]	5	5.2	5.4	5.5	5.3	3.5

and their derivatives under UV light irradiation [1,6,18,22,23]. Because of the rapid recombination of photoexcited electron–hole pairs formed in photocatalytic processes, the photocatalytic efficiency of ZnO is limited. In fact, the recombination has faster kinetics than surface redox reactions and greatly reduces the quantum efficiency of photocatalysis process [20]. To retard the recombination of photoexcited electron––hole pairs and to enhance the photocatalysis efficiency of ZnO, one of the approaches used is to couple ZnO with other materials that act as an electron sink to eliminate or slow down the recombination process of photoinduced electron-hole pairs [20]. Several materials, like carbon nanotube and graphene [20] were used as electron sink to enhance the photocatalytic activity of ZnO. Other papers claimed the use of Fe_3O_4/ZnO/$NiWO_4$ [24] and Fe_3O_4/ZnO/$CoWO_4$ [25] that could improve the separation of the photogenerated charge carriers in the prepared nanocomposites. Moreover, recently it was found that by combining ZnO with other n-type semiconductors, n-n heterojunctions could be formed at the interface of semiconductors [26,27] enhancing the photocatalytic activity of ZnO.

Furthermore, noble metal deposited on ZnO surface, such as Au/ZnO [28], Pt/ZnO [29], Pd/ZnO [30] and Ag/ZnO catalysts [20,31,32] have already found a wide application in the field of photocatalysts. Unlike Au, Pt, and Pd, Ag is cheaper and so Ag/ZnO catalysts have become priority for further scientific investigations and in particular, many methods have been studied to synthesize them such as chemical bath deposition [33], sol–gel method [34], hydrothermal method [35], ultrasonic-assisted method [36] and so on. However, most of these methods of preparation are limited for scientific research purpose because of high temperature, high pressure, expensive equipment, toxic reagents or long reaction time. So, it is necessary to develop a simple and low-cost method to fabricate the Ag/ZnO photocatalysts with high crystallinity. Thus, a simple and fast method for the synthesis of Ag/ZnO catalysts could be the photodeposition method [37–44]. For this reason, in this work silver nanoparticles were reduced and deposited on commercial ZnO surface by using a photodeposition method under UV light irradiation. It was investigated the photocatalytic activity of the prepared Ag/ZnO photocatalysts at different Ag content and compared with the photocatalytic properties of commercial ZnO for the treatment of phenol aqueous solutions. It is worthwhile to note that, at our knowledge, the most papers about Ag/ZnO photocatalysts prepared by photodeposition method were devoted to the degradation of organic dyes [37,38] and only few published studies regard the degradation of phenol [40], showing, in all cases, that the complete removal of phenol was never achieved in less than 3 h of UV irradiation.

2. Experimental

2.1. Synthesis of Ag/ZnO photocatalysts

Ag/ZnO photocatalysts were synthesized through photodeposition method starting from 1 g of commercial ZnO (Aldrich, 99%) suspended into 50 mL of distilled water at room temperature. Different amount of silver nitrate ($AgNO_3$, Aldrich, 99%) was added into the suspension that was irradiated for 30 min by two UV lamps emitting at 365 nm (nominal power of 8 W, Philips). Light intensity on the suspensions was 0.6 W/m^2. A gaseous nitrogen flow (30 NL h^{-1}) was bubbled inside the

suspension during the UV irradiation. In these conditions, oxidation and reduction occur simultaneously in Ag ions photoreduction: in the reduction, the conduction band electrons, generated in the ZnO (e$^-$(CB)) by UV irradiation, can reduce adsorbed Ag$^+$ ions, giving rise to Ag atoms (Ag^0), the reduced Ag^0 is then deposited on the ZnO surface [38]. Photochemical reactions are summarized as follows:

$$ZnO + h\nu \rightarrow e^-(CB) + h^+(VB) \tag{1}$$

$$Ag^+ + e^-(CB) \rightarrow Ag^0 \tag{2}$$

$$2H_2O + h^+(VB) \rightarrow O_2 + 4H^+ \tag{3}$$

After the photodeposition, the suspension was centrifuged, washed with distilled water for several times and finally dried at 90 °C in an oven. The obtained Ag/ZnO photocatalysts will be denoted as x% Ag/ZnO, where x indicates the nominal Ag loading expressed as weight percentage (wt%) (Eq. (4)).

$$\%Ag = \frac{gAg}{gZnO + gAg} \cdot 100 \tag{4}$$

Where:

gAg is the weight of silver calculated from $AgNO_3$ used in the preparation;

$gZnO$ is the weight of commercial ZnO fixed at 1 g and used in the preparation.

Ag/ZnO samples with different Ag loadings were synthesized and these samples are enlisted in Table 1.

2.2. Characterization of the photocatalysts

Different characterization techniques were used to analyze Ag/ZnO photocatalysts. In particular, the specific surface area (SSA) analysis was performed by BET method using N_2 adsorption with a Costech Sorptometer 1042 after a pretreatment at 60 °C for 30 min in He flow (99.9990%). Total Ag loading of the photocatalysts was obtained by X-ray fluorescence spectrometry in a Panalytical Axios sequential spectrophotometer equipped with a rhodium tube as the source of radiation. XRF measurements were performed onto pressed pellets (sample included in 10 wt% of wax).

Silver particles sizes were evaluated by Transmission Electron Microscopy (TEM) in a Philips CM200 instrument, equipped with X-ray EDX X-Max 80T system, Oxford instruments. For this analysis the samples were dispersed in ethanol using an ultrasonicator and dropped on a carbon grid. Determination of the metal particle average diameter in the different samples was accomplished by counting particles in a high number of TEM images from different places of the samples.

X-ray photoelectron spectroscopy (XPS) studies were carried out on a Leybold–Heraeus LHS-10 spectrometer, working with constant pass energy of 50 eV. The spectrometer main chamber, working at a pressure < 2 × 10^{-9} Torr, is equipped with an EA-200MCD hemispherical electron analyzer with a dual X-ray source working with Al K α (hυ = 1486.6 eV) at 120 W and 30 mA C 1 s signal (284.6 eV) was used as internal energy reference in all the experiments. Samples were outgassed in the prechamber of the instrument at 150 °C up to a pressure < 2 × 10^{-8} Torr to remove chemisorbed water.
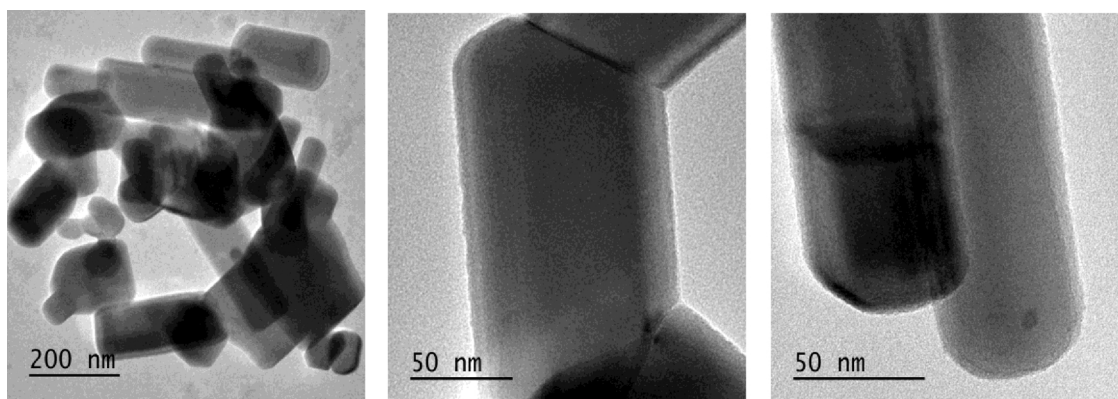
Fig. 1. TEM images of commercial ZnO sample.

The detailed information about the crystalline structure of the photocatalysts was measured by X-ray diffraction analysis (XRD) using Brucker D8 diffractometer and the crystallite sizes were calculated through the Scherrer equation.

The ultraviolet-visible diffuse reflectance spectra (UV–vis DRS) of the samples were recorded using a Perkin Elmer spectrometer Lambda 35 spectrophotometer using a RSA-PE-20 reflectance spectroscopy accessory (Labsphere Inc., North Sutton, NH). The band gap values of photocatalysts were determined through the corresponding Kubelka–Munk function (KM) (which is proportional to the absorption of radiation) and by plotting $(KM \times h\upsilon)^2$ against $h\upsilon$.

2.3. Photocatalytic tests

The photocatalytic activity of commercial ZnO and Ag/ZnO samples was tested under UV irradiation. The photocatalytic tests were conducted in a cylindrical photoreactor (ID = 2.6 cm, L_{TOT} = 41 cm and V_{TOT} = 200 mL) equipped with: (i) an air distributor device (flow rate of 142 Ncc min^{-1}); (ii) four UV lamps (Philips, nominal power: 8 W each and main emission peak at 365 nm) around the external surface of the photoreactor at an equal distance from it (about 30 mm) in order to irradiate the volume of the solution uniformly; (iii) a peristaltic pump (Watson Marlow) in order to maintain continuously recirculated the suspension.

In a typical photocatalytic test, the treated solution volume was 100 mL at the spontaneous pH of the solution (pH = 6.5) with an initial concentration of phenol at 50 mg L^{-1} while the photocatalyst dosage was 1.5 g L^{-1}.

Prior to the irradiation, the suspension was left in dark for 120 min to provide an adsorption/desorption equilibrium on the photocatalyst surface and after, the photocatalytic test was began under UV light irradiation up to 240 min. At different times, about 4 mL of the solution was withdrawn and filtered to remove solid particles powders.

The photodegradation of phenol was monitored by measuring its absorption at 270 nm using a UV Vis spectrophotometer (Evolution 201) [19] while the total organic carbon (TOC) was measured by the high temperature combustion method on a catalyst (Pt-Al$_2$O$_3$) in a tubular flow microreactor operated at 680 °C, with a stream of hydrocarbon free air to oxidize the organic carbon [45].

In this study, photocatalytic activities of the commercial ZnO and prepared Ag/ZnO catalysts was estimated by evaluating the influence of Ag loading on ZnO catalyst, catalyst dosage, initial phenol concentration and finally, a photocatalytic test using the best Ag/ZnO photocatalyst was carried out to treat a drinking water containing phenol.

3. Results and discussion

3.1. Characterization of the photocatalysts

Commercial ZnO and Ag/ZnO photocatalysts were characterized by different techniques such as X-ray fluorescence spectroscopy (XRF), specific surface area (SSA), transmission electron microscopy (TEM), X-ray photoelectron spectroscopy (XPS), X-ray diffraction (XRD) and UV–vis spectroscopy.

3.1.1. XRF results
The total loading of Ag on the photocatalysts prepared was analyzed by XRF measurements (Table 1). As it can be seen, for all the samples, the real Ag content is lower than the nominal Ag loading, thus indicating an incomplete reduction of the metal precursor, however, the Ag content effectively deposited on ZnO increased by increasing the nominal Ag content from 0.14 to 1.28 wt%.

3.1.2. SSA results
SSA results are shown in Table 1. In particular, for Ag/ZnO samples with Ag content in the range of 0.14–0.88 wt%, the SSA values did not change with respect to commercial ZnO (5 m^2 g^{-1}). With the increase of Ag content up to 1.28 wt%, the SSA decreased to 3.5 m^2 g^{-1} indicating a possible agglomeration of the Ag nanoparticles on ZnO surface, previously observed in literature [46].

3.1.3. TEM analysis
Fig. 1 shows selected images of commercial ZnO. The particle sizes were clearly of the order of nanometers (ca.90 nm); this sample exhibited homogeneity on shapes and sizes and there were particles that showed the hexagonal face, along with another type of square or rod-like structures. As it can be seen in Fig. 2, these shapes were maintained after Ag deposition. Silver nanoparticles can be identified as black dots located on ZnO surface. These particles were heterogeneously distributed over the ZnO surface with places with a high concentration of deposits and others relatively empty (Fig. 2). It was found that the number of particles on surface increased with the nominal Ag content. The particle size also increased, thus, for example, for the catalyst prepared with 1.28 wt% of Ag, the average particle size was 3.2 nm. TEM pictures of samples with other metal loadings were not shown for the sake of brevity but they all presented similar morphology and heterogeneous distribution than pictures shown in Fig. 2.

In order to achieve an accurate identification of the silver particles in the samples, EDX analysis were also performed and as it can be observed in Fig. 3, Ag particles are present in the Ag/ZnO samples.

3.1.4. X-ray photoelectron spectroscopy (XPS)
The surface structure of bare and Ag modified ZnO was analyzed by using XPS. Selected spectra of the O1s, Zn 2p and Ag 3d regions
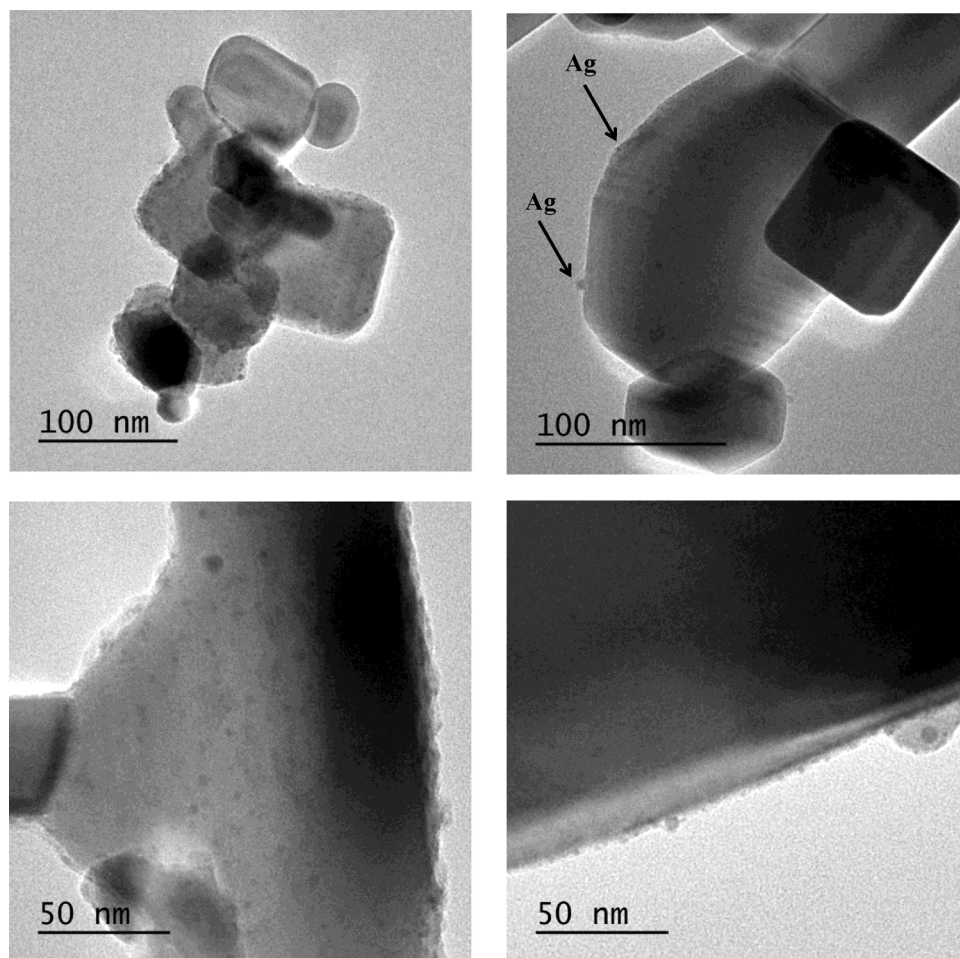
corresponding to the 2%Ag/ZnO sample are shown in Fig. 4. In the obtained spectra, Zn was identified in all the samples by two peaks located at binding energies of 1043 and 1020 eV. In the O 1s region, a peak located at a binding energy of 529.5 ± 0.2 eV was registered in all the samples which was assigned to lattice oxygen in ZnO. No changes in the position of these peaks were observed after Ag addition. In Fig. 4, peaks located at 373 and 367 eV were assigned to Ag $3d_{5/2}$ and Ag $3d_{3/2}$, respectively, corresponding to metallic silver (Ag^0).

3.1.5. X-ray diffraction (XRD)

The XRD analysis was employed to identify the phase structure and the purity of the photocatalysts. The XRD patterns of commercial ZnO and prepared Ag/ZnO photocatalysts were recorded. The results, showed in Fig. 5, evidenced strong diffraction peaks indicating that the synthesized products have high crystallinity. All the prepared samples have the typical hexagonal Wurtzite structure of ZnO [47,48], with 2&z.Theta; diffraction peaks at 31.7°, 34.5°, 36.2°, 47.7°, 56.84°, 63°, 68.1° (Fig. 5) corresponding to (100), (002), (101), (102), (110), (103) and (112) planes, respectively. The maximum diffraction intensity was observed at 36.2°. Ag/ZnO samples revealed three small additional diffraction peaks at 38.2°, 44.2°, and 64.5° that correspond to (111), (200), and (220) crystal planes due to the presence of Ag. These peaks are associated with the face-centered-cubic phase of metallic Ag^0 [38,49,50]. No characteristic peaks of impurity phases, such as silver oxide phases, were observed from the patterns. In addition, there was no remarkable shift of all diffraction peaks indicating that silver atoms are positioned onto the ZnO surface excluding the possibility of their incorporation into the ZnO structure substituting Zn sites [20,46]. Furthermore, the ZnO crystallite size of the samples was calculated using the Debye-Sherrer's formula [39,51] based on the XRD patterns

[39] and considering the diffraction peak at 2θ ~ 36.2° (111). According to the calculations, the average crystallite size of commercial ZnO and Ag/ZnO samples was approximately constant and about 24 nm.

3.1.6. UV–vis diffuse reflectance spectra (UV–vis DRS)

The UV–vis DRS spectra of commercial ZnO and the synthesized 2%Ag/ZnO photocatalyst are shown in Fig. 6. The absorbance spectra (Fig. 6a) evidenced the characteristic absorption edge of the ZnO semiconductor located below 400 nm and also another absorption band, observed in the visible region, for 2%Ag/ZnO photocatalyst. This band is ascribed to the surface plasmon resonance (SPR) absorption of metal silver particles [38,52]. Similar results were obtained for all the Ag/ZnO samples. The data reported in Fig. 6b were used for the evaluation of band gap energy (Table 1) that was found to be approximately 3.1 eV for all the samples, in agreement with literature data [53].

3.2. Photocatalytic activity results

3.2.1. Influence of Ag content photodeposited on ZnO surface

The photocatalytic degradation of phenol under UV light irradiation using commercial ZnO and Ag/ZnO photocatalysts was investigated. The photocatalytic degradation was carried out in a 100 mL of phenol solution with an initial concentration of 50 mg L^{-1} and a catalyst loading of 1.5 g L^{-1}. The experiment results, as a function of irradiation time in terms of phenol degradation and mineralization (Figs. 7 and 8), showed that, in the absence of the photocatalyst (photolysis), the phenol concentration did not change under UV irradiation for 240 min, indicating that the photolysis of phenol can be neglected compared to
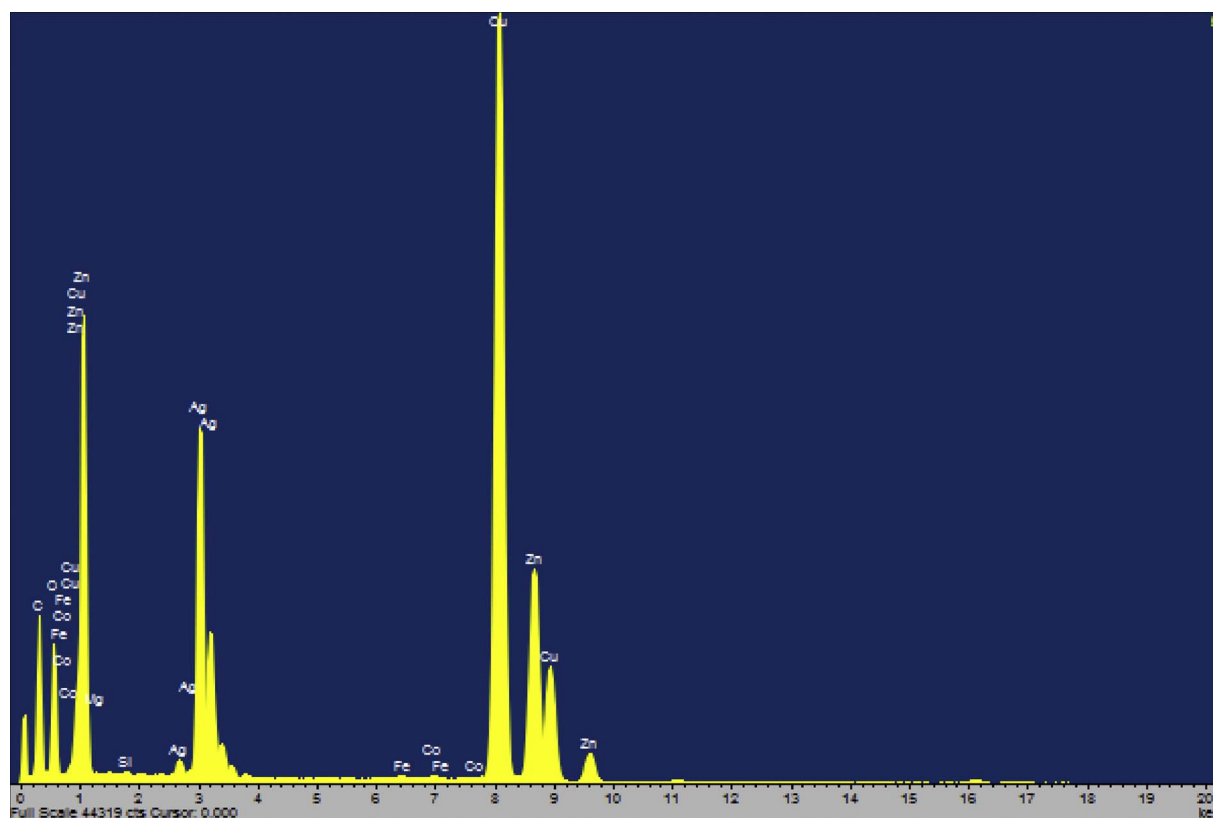
Fig. 3. EDX identification of 2wt%Ag/ZnO sample.

photocatalysis. Figs. 7 and 8 show also the effect of the noble metal Ag photodeposited on the photocatalytic activity of the synthesized catalysts. As it can be seen, the photocatalytic results in terms of phenol degradation (Fig. 7) evidenced a rapidly decrease of phenol concentration in the presence of Ag/ZnO photocatalysts that exhibited enhanced photocatalytic activity compared with the commercial ZnO. In particular, the almost complete phenol degradation was reached after 60 min of irradiation time using 1%Ag/ZnO photocatalyst (Fig. 7). It is worthwhile to note that, at the same irradiation time (60 min), the phenol degradation increased with the increase of Ag content up to 0.88 wt%, while for the highest metal loading (1.28 wt%) the photocatalytic activity of the samples decreased, thus indicating that the optimal Ag content was equal to 0.88 wt%. In the same manner, in terms of TOC removal (Fig. 8), the optimal silver loading was found to be 0.88 wt%. In fact, 1%Ag/ZnO photocatalyst was able to achieve the total TOC removal after 120 min of UV light irradiation. The existence of an optimal silver content indicates that an appreciable amount of Ag is necessary to reach the maximum improvement of the photocatalytic activity [38,40]. The improvement of commercial ZnO by modifying its surface with Ag can be explained taking into account the characterization results previously described. Thus, the addition of Ag to ZnO, leads to modify the color of this material, leading to improve the absorption of the metalized samples in the visible region as it can be observed by UV–vis DRS analysis, where the SPR of silver was detected (Fig. 6). By TEM analysis it was also observed that the increase of the metal content leads to increase the number of Ag nanoparticles deposited in ZnO surface. However, the biggest silver nanoparticles, present in the catalyst prepared with 1.28 wt% Ag, can act as a recombination centers, thus leading to decrease the photocatalytic activity of this material, as it can be observed in the present study. On the other hand, taking into account that the Ag reduction on ZnO surfaces was incomplete in all the prepared photocatalysts, as it was observed by XRF analysis (Table 1), it is expected a certain contribution of Ag oxidized species in the samples prepared with the lowest silver content (i.e

0.14–0.88 wt%). However, it was not possible to calculate the percentage of Ag^0 or $Ag^{\delta+}$ species for these samples, as the ratio signal to noise was too low to allow an accurate enough estimation by XPS. In the case of the samples prepared with 1.28 wt% of Ag, only signals corresponding to metallic species (Ag^0) was identified in the Ag 3d region (Fig. 4). In previous studies it has been reported that the oxidized species of metals such as platinum ($Pt^{\delta+}$) can act as additional adsorption centers for phenol (as a bidentate phenolate) on the semiconductor surface [54], thus leading to improve the substrate adsorption and therefore to increase the effectiveness of the phenol photodegradation over photocatalyst metallized by photodeposition method. A similar behavior can occur in the case of the silver ZnO modified photocatalysts studied in the present work. Thus, the increase of the Ag content to 1.28 wt% led also to increase the Ag^0 species effectively deposited on ZnO surface, as it can be observed by XPS (Fig. 4) and therefore to decrease the available adsorption centers for phenol ($Ag^{\delta+}$). This reason can contribute to explain why the phenol photodegradation decreased over the 2%Ag/ZnO sample (Fig. 7).

In order to understand the influence of silver content on photocatalytic activity, the kinetic constant of phenol degradation was evaluated. For this purpose it was considered that the phenol photodegradation reaction follows the pseudo-first-order kinetic [55]. The photodegradation rate (r) depends on the phenol concentration (C) in accordance with the following equation Eq. (5):

$$r = k \cdot C \qquad (5)$$

Where C is the concentration of phenol in mg L^{-1} and k is the kinetic constant in min^{-1}.

Considering the mass balance on phenol (Eq. (6)) and integrating it between initial time (t = 0) and a generic irradiation time t, it was obtained the equation Eq. (7).

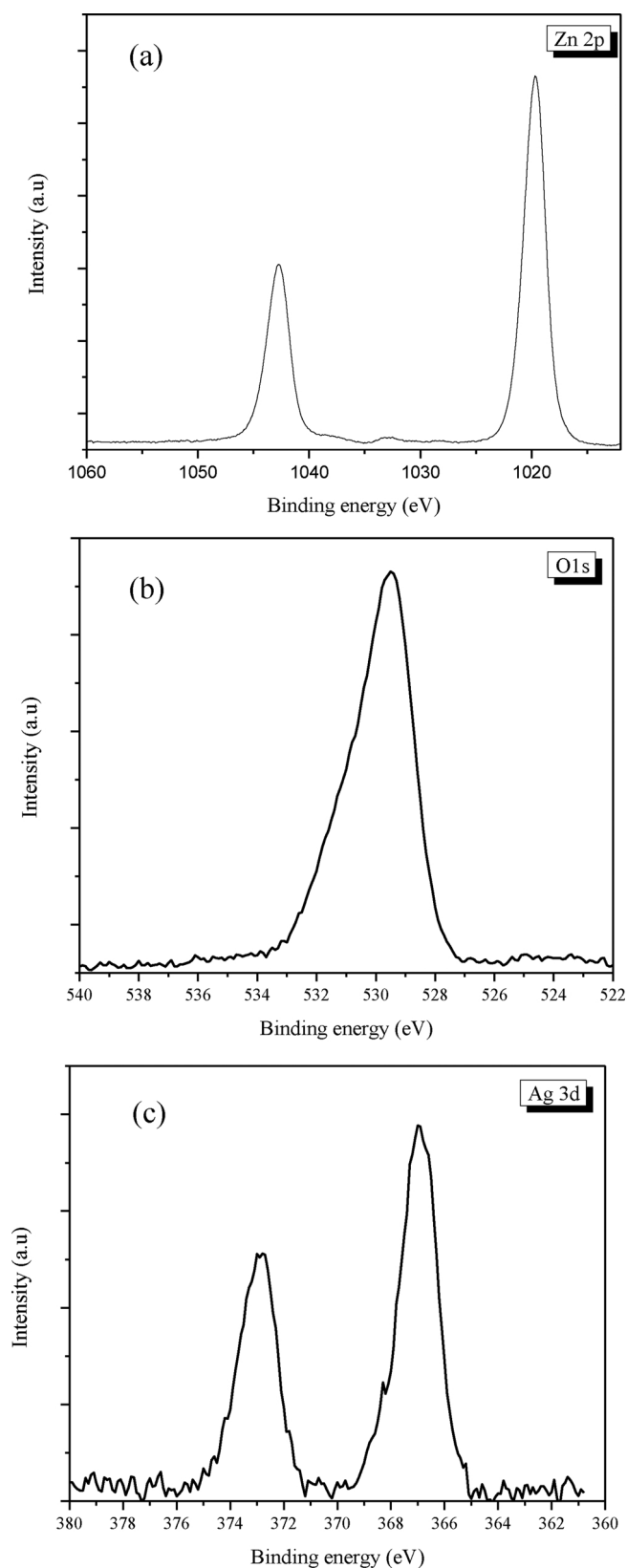$$\frac{dC}{dt} = -k \cdot C \qquad (6)$$

Fig. 4. XPS core level spectra of Zn 2p (a), O 1s (b) and Ag 3d (c) regions for 2wt%Ag/ZnO sample.

$$-\ln\left(\frac{C}{C_0}\right) = k \cdot t \qquad (7)$$

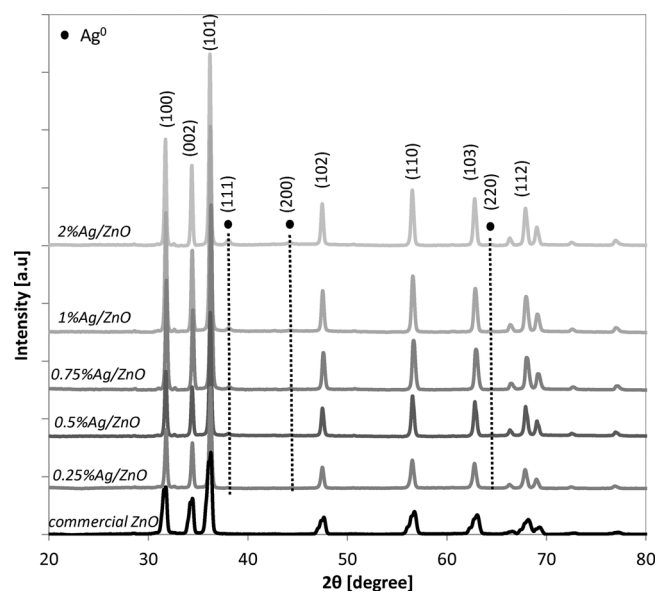The value of the kinetic constant k can be calculated by the slope of

Fig. 5. XRD patterns of commercial ZnO and Ag/ZnO photocatalysts in the range 20–80°.

the straight line obtained by plotting $-\ln\left(\frac{C}{C_0}\right)$ versus irradiation time (t). The obtained values of k for all the investigated photocatalysts were reported in Fig. 9. As it can be seen in this figure, the k values of all Ag/ZnO samples were higher than the calculated for commercial ZnO. The reason of this result could be attributed to the presence of Ag on ZnO surface that effectively inhibits the recombination of photoinduced electron and hole pairs, as reported in literature [40]. This observation was confirmed by UV–vis DRS spectra (Fig. 6) in which it was evidenced the presence of SPR absorption. Possibly, due to SPR and synergetic effect of the Ag particles, a large number of photoexcited electrons was generated from the Ag particles surfaces to the conduction band of ZnO and diffuse into the surrounding medium, consequently increasing the photocatalytic activity [53]. With regard to the influence of metal loading, it is possible to observe that, with the increase of Ag content, the kinetic constant value increased progressively up to Ag content equal to 0.88 wt%, while with higher content of Ag, the k values begun to decrease. It is clear that the best photocatalyst was 1%Ag/ZnO because it exhibited the highest value of k and so the phenol photodegradation took place more rapidly than the other photocatalysts with a different content of silver. It can be seen that, once again, there was an optimized amount of Ag photodeposited on ZnO. In fact, for Ag content higher than 0.88 wt%, Ag particles may become the center for recombining photoinduced electron and hole pairs and so the photoactivity of photocatalysts began to decrease [38,40]. Moreover, it is worthwhile to note that the obtained kinetic constant value for 1%Ag/ZnO photocatalyst was significantly higher than the values reported in the scientific literature regarding phenol photodegradation using ZnO modified with Ag through a photodeposition method [40].

From these results, it is evident that the best photocatalyst is 1%Ag/ZnO. This sample was chosen to investigate the influence of photocatalyst dosage and the change of the initial phenol concentration in solution.

3.2.2. Influence of 1%Ag/ZnO dosage

The experiments were carried out using different catalyst amounts (in the range 0.075–0.3 g) in 100 mL aqueous solution, while the initial phenol concentration was kept constant at 50 mg·L^{-1}. The results, as a function of irradiation time, in terms of phenol degradation and TOC removal were reported in Figs. 10 and 11, respectively. It can be noted that the photocatalytic activity of 1%Ag/ZnO gradually improved with the increase of its dosage from 0.075 to 0.15 g while with higher dosage (0.3 g), the photocatalytic performances did not change reaching the
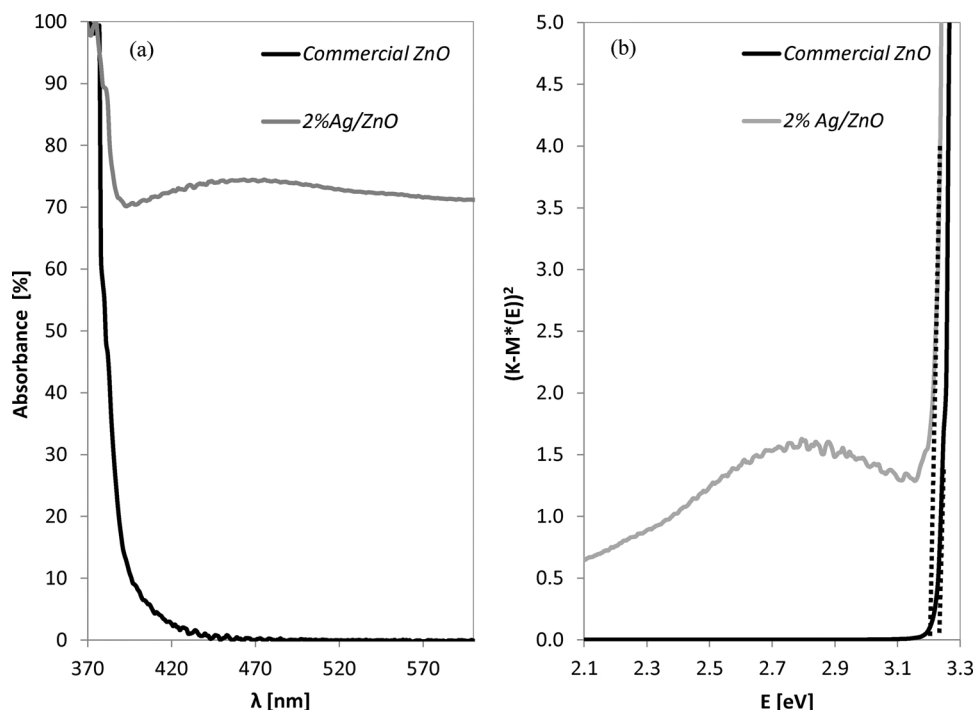
Fig. 6. UV–vis Diffuse Reflectance Spectra of commercial ZnO and 2%Ag/ZnO photocatalyst (a) and band-gap evaluation (b).

complete phenol degradation after 120 min of UV light irradiation. This last result indicates that the turbidity of the suspension did not induce a decrease of photocatalytic performances. In the same manner, Fig. 11 shows the results in terms of mineralization of organic compound after 45 min of UV light irradiation. In particular, the value of TOC removal increased with the increase of 1%Ag/ZnO amount from 0.075 to 0.15 g and then it stayed constant (68%) for 1%Ag/ZnO dosage equal to 0.3 g. Both photocatalytic phenol degradation and mineralization did not change significantly when the photocatalyst dosage was increased up to 0.3 g, and so it is economically cheap to use the smaller amount of the photocatalyst (0.15 g).

3.2.3. Influence of phenol initial concentration

The effect of phenol initial concentration in the range

$12.5–50 \, mg \, L^{-1}$, has been investigated by using 0.15 g of 1%Ag/ZnO. In particular, Figs. 12 and 13 show the results in terms of phenol degradation and TOC removal as a function of irradiation time, respectively. With regard to the photocatalytic phenol degradation (Fig. 12), the activity of the 1%Ag/ZnO photocatalyst remained unchanged also in presence of high initial phenol concentration, reaching the complete degradation after 120 min of UV light irradiation for all photocatalytic tests. From the comparison of the results in terms of TOC removal (Fig. 13) after 45 min of UV light irradiation, it can be seen the TOC removal values did not change significantly with the increase of the initial phenol concentration. Moreover, the k values were obtained and the results (Fig. 14) showed that, with the increase of the initial phenol concentration, there is no influence on the kinetic constant value. These results are in contrast with the most papers dealing with the
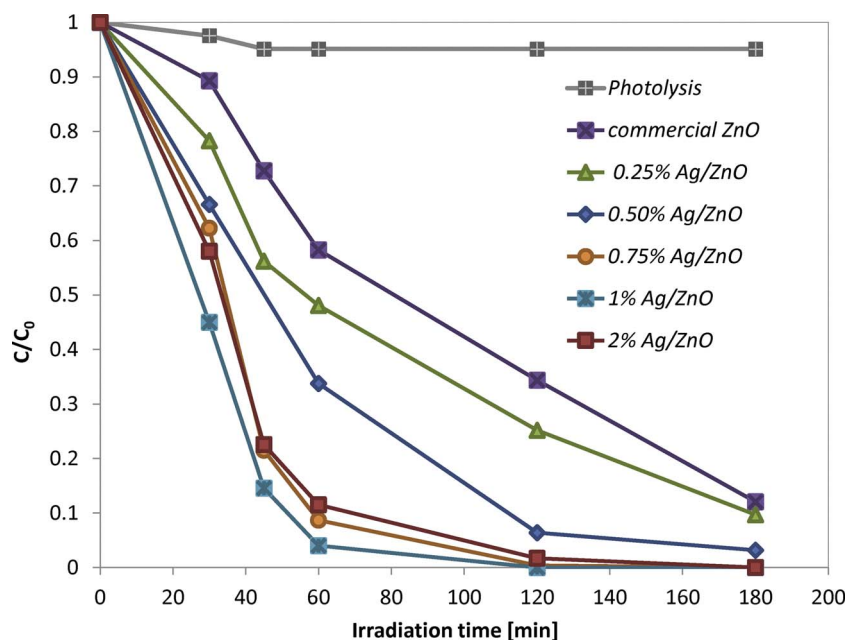
Fig. 7. Photocatalytic phenol degradation under UV light using commercial ZnO and Ag/ZnO photocatalysts; phenol initial concentration: $50 \, mg \, L^{-1}$; photocatalyst dosage: $1.5 \, g \, L^{-1}$.
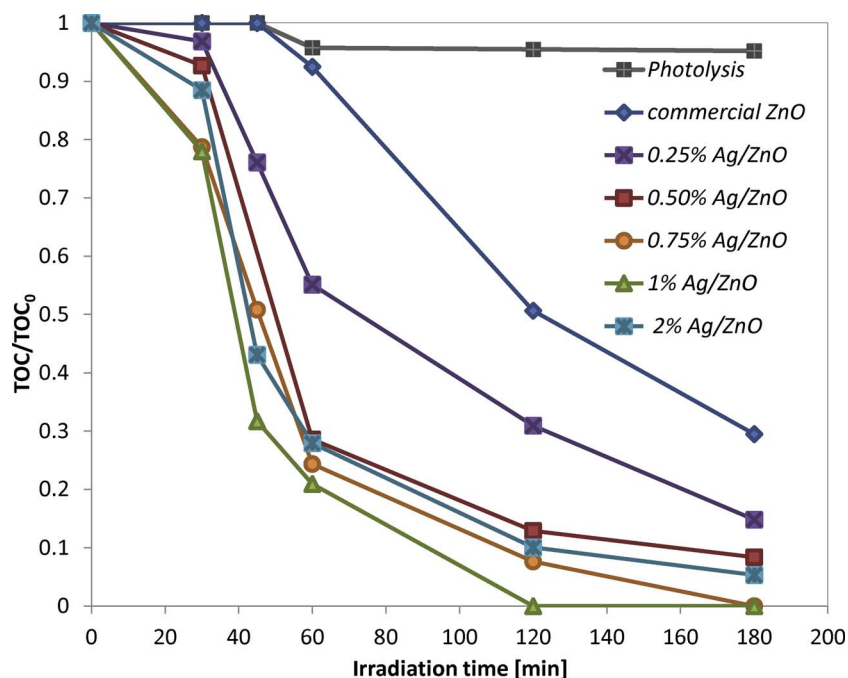
Fig. 8. Total Organic Carbon (TOC) behavior under UV light using commercial ZnO and Ag/ZnO photocatalysts; phenol initial concentration: 50 mg L^{-1}; photocatalyst dosage: 1.5 g L^{-1}.
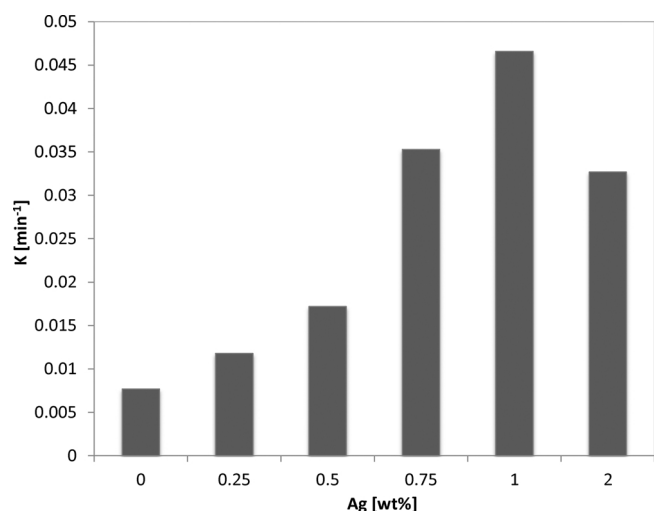

Fig. 9. Kinetic constants for phenol degradation using commercial ZnO and Ag/ZnO photocatalysts under UV light; phenol initial concentration: 50 mg L^{-1}; photocatalyst dosage: 1.5 g L^{-1}.

Fig. 10. Photocatalytic phenol degradation under UV light using different 1%Ag/ZnO photocatalyst dosage; phenol initial concentration: 50 mg L^{-1}; solution volume: 100 mL.

photocatalytic degradation of phenol [6] in which it was shown that the degradation efficiency of phenol decreased when the initial pollutant concentration increased, possibly due to the formation of intermediates strongly adsorbed on photocatalyst surface. Therefore, our 1%Ag/ZnO photocatalyst could be able to degrade phenol and intermediates in an effective way, as evinced from TOC data (Fig. 13), allowing to treat aqueous solutions in the presence of also high phenol initial concentration and without changing significantly the kinetic of photocatalytic reaction.

3.2.4. Photocatalytic test on a drinking water matrix containing phenol

Photocatalytic test was performed by using 0.15 g of the otimized catalyst (1%Ag/ZnO) to treat a drinking water containing phenol with an initial concentration at 50 mg L^{-1} in 100 mL aqueous solution. The physic-chemical characteristics of the treated drinking water are reported in Table 2.

Fig. 15 shows the comparison between photocatalytic tests in presence of distilled water and a drinking water in terms of phenol
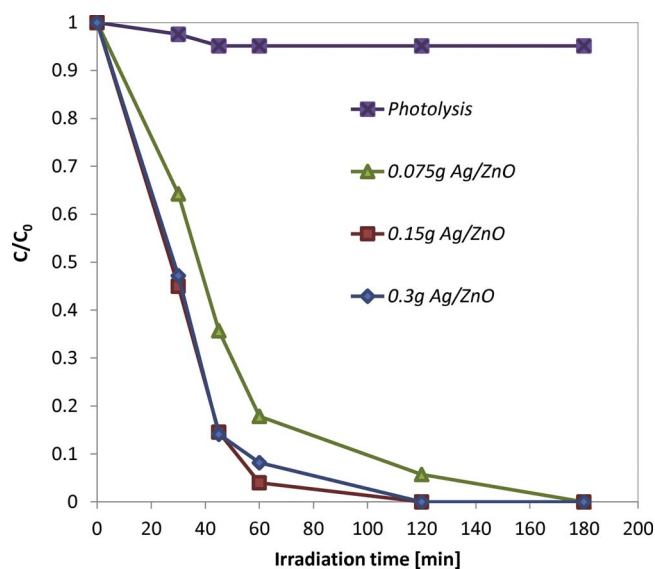
degradation and mineralization of the organic substance, in the same experimental conditions. It can be observed that the phenol removal rate was lower for the real matrix because of the presence of ions scavengers in solution such as carbonates, chlorides and nitrates (Table 2) which are capable to sequestrate a part of the radical species formed during UV light irradiation. However, the total phenol degradation (Fig. 15) with the almost complete mineralization for the drinking water was reached after 180 min of UV irradiation time. These results evidence the possibility of using the developed photocatalytic system for the treatment of waters containing phenol in order to reuse them since are respected the limit values (lower than 0.5 mg L^{-1}) imposed by the Italian Legislation (D.Lgs. 152/06) allowed in the final effluent.

4. Conclusions

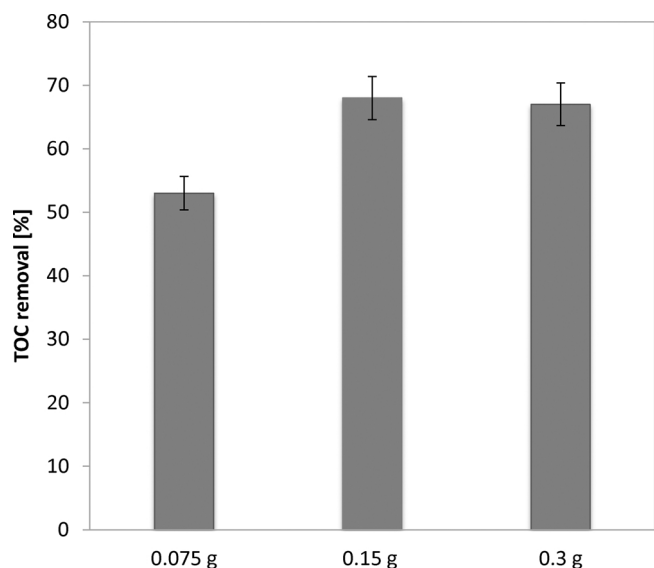In this work the photocatalytic activity of Ag/ZnO photocatalysts

Fig. 11. TOC removal after 45 min of UV irradiation using different 1%Ag/ZnO dosage; phenol initial concentration: 50 mg L^{-1}; solution volume: 100 mL.
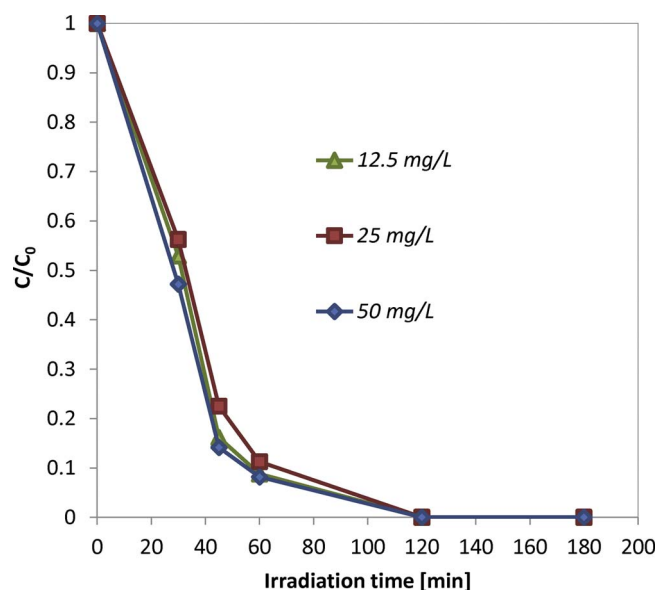

Fig. 13. TOC removal after 45 min of UV irradiation at different initial phenol concentration using 1%Ag/ZnO photocatalyst; photocatalyst dosage: 1.5 g L^{-1}.

Fig. 12. Photocatalytic phenol degradation under UV light at different initial phenol concentration using 1%Ag/ZnO photocatalyst; photocatalyst dosage: 1.5 g L^{-1}.

Fig. 14. Kinetic constants after 45 min of UV irradiation at different initial phenol concentration using 1%Ag/ZnO photocatalyst; photocatalyst dosage: 1.5 g L^{-1}.

Table 2
Chemical-physical characteristics of the drinking water matrix.

	mg L^{-1}
HCO_3^-	249
Ca^{2+}	59.80
Mg^{2+}	12.90
Cl^-	6
NO_3^-	7.10
SO_4^{2-}	3.40
Na^+	3.16
K^+	1.08
F^-	0.076

was investigated for the treatment of aqueous solutions containing phenol under UV light irradiation. Ag/ZnO samples were synthetized by photodeposition method and they were characterized by different techniques. The obtained results evidenced that ZnO was present as hexagonal wurtzite phase and Ag, present as metallic silver (Ag^0), was successfully deposited on ZnO surface. It was found that Ag content effectively deposited on ZnO increases by increasing the nominal Ag content from 0.14 to 1.28 wt%. Moreover UV–vis DRS spectra showed that Ag/ZnO samples revealed a reflectance band ascribed to the surface plasmon resonance (SPR) absorption of metal silver particles. The silver loading used in the preparation of Ag/ZnO photocatalysts is an important factor influencing the physicochemical properties of the obtained photocatalyst. It was observed an enhancement of photocatalytic phenol removal under UV light irradiation from aqueous solutions by silver addition in comparison to commercial ZnO. In fact, the highest photocatalytic phenol removal from aqueous solution was obtained by using 1%Ag/ZnO as photocatalyst, confirmed also by the evaluation of the kinetic constant for phenol degradation. In particular,
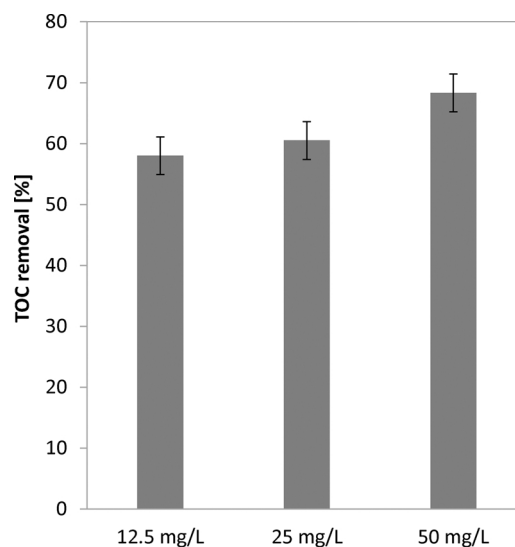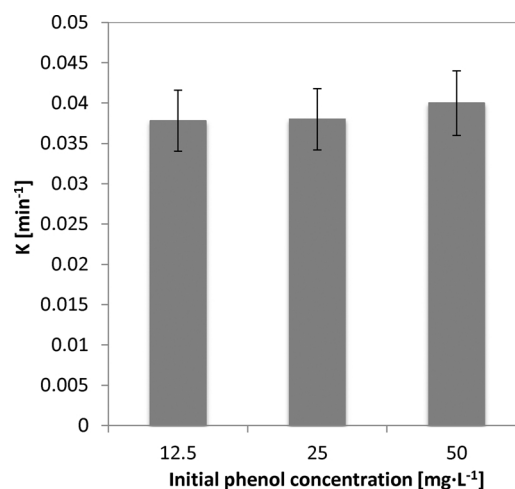
1%Ag/ZnO was able to achieve both the total phenol degradation and the total TOC removal in 120 min of UV light irradiation. This enhancement can be explained by the presence of the SPR of silver observed by UV–vis spectra indicating that a large number of photoexcited electrons were generated from the Ag particles surfaces to the conduction band of ZnO, consequently increasing the photocatalytic activity. With a content of Ag higher than 0.88 wt%, the biggest number of Ag particles can obstruct the active sites on ZnO surface worsening
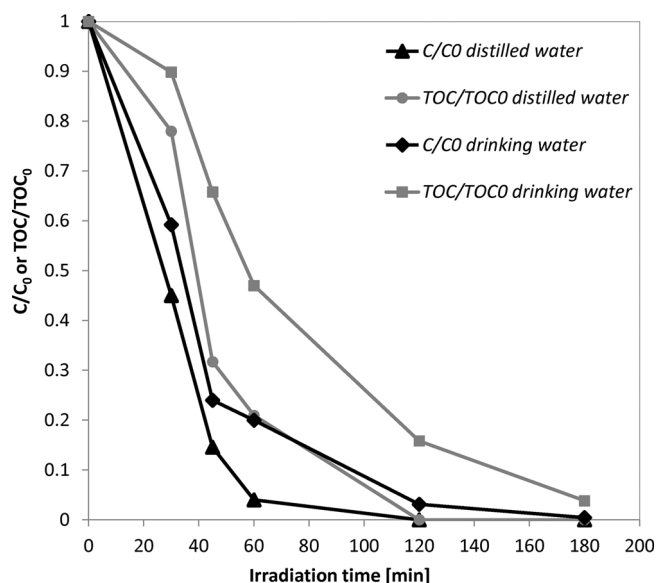
Fig. 15. Photocatalytic phenol degradation and mineralization of a drinking water and distilled water under UV light with 1% Ag/ZnO photocatalyst; phenol initial concentration: 50 mg L^{-1}; photocatalyst dosage: 1.5 g L^{-1}.

the photocatalytic performances. As it can be observed by XPS, the increase of the Ag content to 1.28 wt% led also to increase the Ag^0 species effectively deposited on ZnO surface, and therefore to decrease the available adsorption centers for phenol (Ag$^{\delta+}$). The optimized phototocatalyst was also able to treat a real drinking wastewater containing phenol; in fact, both the total phenol degradation and the almost complete mineralization was reached using 1%Ag/ZnO photocatalyst after 120 min of UV irradiation. At last, 1%Ag/ZnO photocatalyst was tested in the treatment of a real drinking wastewater containing phenol in which the total phenol removal after 180 min of UV irradiation time was achieved confirming the possibility to employ the in the treatment of real wastewater.

Acknowledgements

References

[1] H. Benhebal, M. Chaib, T. Salmon, J. Geens, A. Leonard, S.D. Lambert, M. Crine, B. Heinrichs, Alex. Eng. J. 52 (2013) 517–523.
[2] F. Delval, G. Crini, J. Vebrel, Bioresour. Technol. 97 (2006) 2173–2181.
[3] O.M. Ontañon, P.S. González, G.G. Barros, E. Agostini, New Biotechnol. 37 (2017) 172–179.
[4] D. Lu, Y. Zhang, S. Niu, L. Wang, S. Lin, C. Wang, W. Ye, C. Yan, Biodegradation 23 (2012) 209–219.
[5] B. Chakraborty, S. Indra, D. Hazra, R. Betai, L. Ray, S. Basu, BioMed Res. Int. 2013 (2013).
[6] J. Ye, X. Li, J. Hong, J. Chen, Q. Fan, Mater. Sci. Semicond. Process. 39 (2015) 17–22.
[7] D. Liu, Z. Zheng, C. Wang, Y. Yin, S. Liu, B. Yang, Z. Jiang, J. Phys. Chem. C 117 (2013) 26529–26537.
[8] E.M. Seftel, M.C. Puscasu, M. Mertens, P. Cool, G. Carja, Appl. Catal. B: Environ. 150–151 (2014) 157–166.
[9] A. Bhattacharya, A. Gupta, A. Kaur, D. Malik, Appl. Microbiol. Biotechnol. 98 (2014) 9829–9841.
[10] Y.K. Ooi, L. Yuliati, S.L. Lee, Chin. J. Catal. 37 (2016) 1871–1881.
[11] H. Barndõk, D. Hermosilla, C. Han, D.D. Dionysiou, C. Negro, Á. Blanco, Appl. Catal. B: Environ. 196 (2016) 232.
[12] S. Weon, W. Choi, Environ. Sci. Technol. 50 (2016) 2556–2563.
[13] C. Wang, H. Zhang, F. Li, L. Zhu, Environ. Sci. Technol. 44 (2010) 6843–6848.
[14] K. Yu, S. Yang, C. Liu, H. Chen, H. Li, C. Sun, S.A. Boyd, Environ. Sci. Technol. 46 (2012) 7318–7326.
[15] X.Z. Li, H. Liu, L.F. Cheng, H.J. Tong, Environ. Sci. Technol. 37 (2003) 3989–3994.
[16] C. Yu, W. Zhou, H. Liu, Y. Liu, D.D. Dionysiou, Chem. Eng. J. 287 (2016) 117–129.
[17] V. Vaiano, O. Sacco, G. Iervolino, D. Sannino, P. Ciambelli, R. Liguori, E. Bezzeccheri, A. Rubino, Appl. Catal. B: Environ. 176–177 (2015) 594–600.
[18] F.C.S. Paschoalino, M.P. Paschoalino, E. Jordao, W.d.F. Jardim, Open J. Phys. Chem. 2 (2012) 135–140 136 pp.
[19] A.K.L. Sajjad, S. Shamaila, B. Tian, F. Chen, J. Zhang, Appl. Catal. B: Environ. 91 (2009) 397–405.
[20] F. Sun, X. Qiao, F. Tan, W. Wang, X. Qiu, J. Mater. Sci. 47 (2012) 7262–7268.
[21] V. Vaiano, M. Matarangolo, O. Sacco, D. Sannino, Appl. Catal. B: Environ. 209 (2017) 621–630.
[22] E. Grabowska, J. Reszczyńska, A. Zaleska, Water Res. 46 (2012) 5453–5471.
[23] A.B. Ahmed, B. Jibril, S. Danwittayakul, J. Dutta, Appl. Catal. B: Environ. 156–157 (2014) 456–465.
[24] A. Habibi-Yangjeh, M. Shekofteh-Gohari, Sep. Purif. Technol. 184 (2017) 334–346.
[25] M. Shekofteh-Gohari, A. Habibi-Yangjeh, Ceram. Int. 43 (2017) 3063–3071.
[26] M. Shekofteh-Gohari, A. Habibi-Yangjeh, RSC Adv. 6 (2016) 2402–2413.
[27] M. Kevin, Y.H. Fou, A.S.W. Wong, G.W. Ho, Nanotechnology 21 (2010).
[28] B. Donkova, P. Vasileva, D. Nihtianova, N. Velichkova, P. Stefanov, D. Mehandjiev, J. Mater. Sci. 46 (2011) 7134–7143.
[29] P. Pawinrat, O. Mekasuwandumrong, J. Panpranot, Catal. Commun. 10 (2009) 1380–1385.
[30] Y. Chang, J. Xu, Y. Zhang, S. Ma, L. Xin, L. Zhu, C. Xu, J. Phys. Chem. C 113 (2009) 18761–18767.
[31] C. Jaramillo-Páez, J.A. Navío, M.C. Hidalgo, M. Macías, Catal. Today 284 (2017) 121–128.
[32] M. Pirhashemi, A. Habibi-Yangjeh, Ceram. Int. 43 (2017) 13447–13460.
[33] Y.F. Wang, J.H. Yao, G. Jia, H. Lei, Acta Phys. Pol. A 119 (2011) 451–454.
[34] Y. Lu, Y. Lin, D. Wang, L. Wang, T. Xie, T. Jiang, J. Phys. D: Appl. Phys. 44 (2011).
[35] W. Lu, S. Gao, J. Wang, J. Phys. Chem. C 112 (2008) 16792–16800.
[36] M. Pirhashemi, A. Habibi-Yangjeh, J. Colloid Interface Sci. 491 (2017) 216–229.
[37] H.F. Yu, D.W. Qian, Part. Sci. Technol. 33 (2015) 197–203.
[38] N.N.K. Truong, T.N. Trung, N. Tu, N.V. Nghia, D.M. Thuy, Int. J. Nanotechnol. 10 (2013) 260–268.
[39] Y. Chen, W.H. Tse, L. Chen, J. Zhang, Nanoscale Res. Lett. 10 (2015).
[40] J. Liqiang, W. Dejun, W. Baiqi, L. Shudan, X. Baifu, F. Honggang, S. Jiazhong, J. Mol. Catal. A: Chem. 244 (2006) 193–200.
[41] D. Sannino, V. Vaiano, P. Ciambelli, M.C. Hidalgo, J.J. Murcia, J.A. Navío, J. Adv. Oxid. Technol. 15 (2012) 284–293.
[42] V. Vaiano, G. Iervolino, G. Sarno, D. Sannino, L. Rizzo, J.J. Murcia Mesa, M.C. Hidalgo, J.A. Navío, Oil Gas Sci. Technol. 70 (2015) 891–902.
[43] G. Iervolino, V. Vaiano, J.J. Murcia, L. Rizzo, G. Ventre, G. Pepe, P. Campiglia, M.C. Hidalgo, J.A. Navío, D. Sannino, J. Catal. 339 (2016) 47–56.
[44] T.J. Wong, F.J. Lim, M. Gao, G.H. Lee, G.W. Ho, Catal. Sci. Technol. 3 (2013) 1086–1093.
[45] D. Sannino, V. Vaiano, P. Ciambelli, L.A. Isupova, Chem. Eng. J. 224 (2013) 53–58.
[46] K. Saoud, R. Alsoubaihi, N. Bensalah, T. Bora, M. Bertino, J. Dutta, Mater. Res. Bull. 63 (2015) 134–140.
[47] X. Zhang, J. Qin, Y. Xue, P. Yu, B. Zhang, L. Wang, R. Liu, Sci. Rep. 4 (2014).
[48] P.R. Deshmukh, Y. Sohn, W.G. Shin, J. Alloys Compd. 711 (2017) 573–580.
[49] M. Arab Chamjangali, G. Bagherian, A. Javid, S. Boroumand, N. Farzaneh, Spectrochim. Acta – Part A: Mol. Biomol. Spectrosc. 150 (2015) 230–237.
[50] Y. Zheng, L. Zheng, Y. Zhan, X. Lin, Q. Zheng, K. Wei, Inorg. Chem. 46 (2007) 6980–6986.
[51] A.L. Patterson, Phys. Rev. 56 (1939) 978–982.
[52] X. Zhang, Y. Wang, F. Hou, H. Li, Y. Yang, X. Zhang, Y. Yang, Y. Wang, Appl. Surf. Sci. 391 (2017) 476–483.
[53] B. Sarma, B. Sarma, Appl. Surf. Sci. 410 (2017) 557–565.
[54] J.J. Murcia, M.C. Hidalgo, J.A. Navío, J. Araña, J.M. Doña-Rodríguez, Appl. Catal. B: Environ. 150–151 (2014) 107–115.
[55] H. Al-Ekabi, N. Serpone, J. Phys. Chem. 92 (1988) 5726–5731.